# Coupling Analysis and Control of a Turboprop Engine

C. Le Brun[1], E. Godoy[1], D. Beauvois[1], B. Liacu[2] and R. Noguera[3]
[1]*Automatic Control Department, Supelec, Gif-sur-Yvette, France*
[2]*Systems Division, SNECMA (SAFRAN), Villaroche, France*
[3]*DynFluid Laboratory, Arts & Métiers ParisTech, Paris, France*

Keywords: TITO Processes, Multivariable Control, Decentralized Control, Turboprop Engine, Interaction Analysis, Decoupling Methods, Mu-Analysis.

Abstract: The goal of this paper is to describe the different steps of the decentralized control design applied on a turboprop engine. An important part of the present approach is the interaction analysis, which leads to the choice of a decentralized strategy with a full compensator. After designing the control laws, the structured singular value approach has allowed to validate the robustness of these. Control laws have finally been interpolated before implementation on the non-linear simulation model of turboprop engine.



## 1 INTRODUCTION

Most of the industrial processes are multivariable in nature. In such systems, each manipulated variable may affect several controlled variables, causing interaction between the loops. In many practical situations, the design of a full MIMO (Multiple-Input Multiple-Output) controller is cumbersome and high-order controllers are generally obtained. The decentralized strategy consists in dividing the MIMO process into a combination of several SISO (Single-Input Single-Output) processes and to design monovariable controllers in order to drive the MIMO process. Due to important benefits, such as flexibility as well as design simplicity, decentralized control design techniques are largely preferred in industry and particularly on turboprop engines (High, et al., 1991). This paper is an extension of (Le Brun, et al., 2014) which presents a preliminary study of an alternative control solution for a turboprop engine.

This paper is organized as follows: Section 2 introduces the turboprop engine and its functioning. The interaction analysis is then presented in Section 3. Section 4 and 5 expose the decoupling techniques and the PID tuning. Robustness analysis and simulation results demonstrate the efficiency of the control laws in Section 6 and 7 before presenting conclusions and perspectives in Section 8.

## 2 FUNCTIONING OF A TURBOPROP ENGINE

### 2.1 Turboprop Overview

Basically, a turboprop engine (Soares, 2008) includes an intake, compressors, a combustor, turbines, a reduction gearing and a variable pitch propeller. Air is drawn into the intake and compressed until it reaches the desired pressure, speed and temperature. Fuel is then injected to the compressed air in the combustor, where the fuel-air mixture is combusted. The hot combustion gases expand through the turbine. The power generated by the turbine is transmitted through the reduction gearing to the propeller, which generates the thrust of the turboprop engine. Thanks to the variable pitch, the propeller turns at constant speed.

From the control point of view, the turboprop engine (Snecma, 2012) is a TITO (Two-Input Two-Output) process. The fuel flow $WF$ is used to control the shaft power $SHP$, while the blade pitch angle $\beta$ is used to control the propeller speed $XNP$. In case of fuel flow changes, the propeller speed is impacted and similarly, when varying the blade pitch angle to change the propeller speed to another level, the shaft power is affected, particularly during the transient states. Fast transitions may generate over-torques with damaging mechanical impacts.


Le Brun C., Godoy E., Beauvois D., Liacu B. and Noguera R..
Coupling Analysis and Control of a Turboprop Engine.
DOI: 10.5220/0005575904200427
In *Proceedings of the 12th International Conference on Informatics in Control, Automation and Robotics* (ICINCO-2015), pages 420-427
ISBN: 978-989-758-122-9

### 2.2 Technical Specifications

Technical specifications are described in Table 1. ***Note:*** *the desired bandwidth and the axis of all figures in this paper will be normalized.*

Table 1: Technical specifications.

| Loop | Bandwidth | Stability Margin | Overshoot |
|---|---|---|---|
| *SHP* | $\omega_{c1}=2\times10^{-2}$ | 45°-6dB | 1% |
| *XNP* | $\omega_{c2}=5\times10^{-2}$ | 45°-6dB | 5% |

Beside these technical specifications, couplings between loops have to be reduced as much as possible and control laws have to be robust to model uncertainties. Moreover, if modifications are required following bench tests or objectives updates, the control laws have to be easily tunable. To respect these last objectives, a decentralized strategy has been chosen. The following notations are used: $G_o$ is the static gain matrix of the process $G$, and $G^*$ is the matrix composed of the diagonal elements of $G$.

### 2.3 Plant Identification

The behavior of the turboprop engine depends on the altitude, the Mach number and the engine rotation speed. A numerical identification has been done at different operating points using a complete non-linear simulator of the turboprop engine. Linear discrete models of second order have been determined to represent the behavior of the turboprop (1), (2). The sampling time $T_e$ has been taken in agreement with the digital electronic unit of the engine. Bode diagrams of the identified models are represented in Fig. 1.

$$\begin{bmatrix} SHP[k+1] \\ XNP[k+1] \end{bmatrix} = \begin{bmatrix} A_{11} & A_{12} \\ A_{21} & A_{22} \end{bmatrix} \begin{bmatrix} SHP[k] \\ XNP[k] \end{bmatrix} + \begin{bmatrix} B_{11} & B_{12} \\ B_{21} & B_{22} \end{bmatrix} \begin{bmatrix} WF[k] \\ \beta[k] \end{bmatrix} \quad (1)$$

$$\begin{bmatrix} SHP \\ XNP \end{bmatrix} = \frac{1}{(z-p_1)(z-p_2)} \begin{bmatrix} K_{11}(z-z_{11}) & K_{12}(z-z_{12}) \\ K_{21}(z-z_{21}) & K_{22}(z-z_{22}) \end{bmatrix} \begin{bmatrix} WF \\ \beta \end{bmatrix} \quad (2)$$

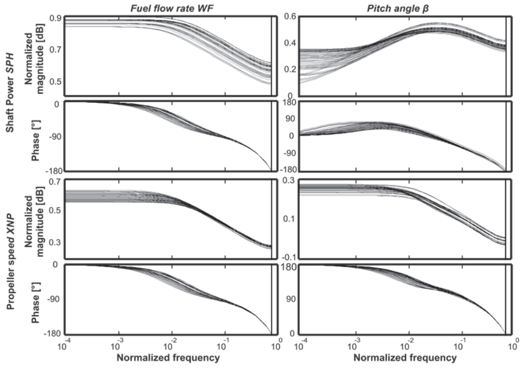


Figure 1: Bode diagrams of the identified models.

# 3 INTERACTION ANALYSIS

### 3.1 Objectives of the Analysis

For significant interactions, a decentralized control may not be adapted due to its limited structure. Thus, it is important to study the practical aspects of a decentralized control when evaluating the interaction level. This last strongly depends on the loop configuration, ie. the manner in which the manipulated variables and the controlled variables have been associated.

Once the decentralized control and the loop configuration have been chosen, the second step is to design the monovariable controllers for each loop. It is possible to use single-loop or multi-loop design methods. The first ones do not take into account the interactions and do not guarantee the performances of the multivariable closed-loop system. The second ones take into account the interactions but are more cumbersome. It can thus be interesting to have a metric to evaluate if a multi-loop tuning method is necessary or not.

If a decentralized control seems not appropriate, a decoupling network can be used to reduce the existing process interactions before designing a decentralized controller. The choice of the structure and the computation of the decoupling network depend on the level of interaction.

A metric is thus needed when a decentralized control is studied.

### 3.2 Proposed Procedure

Despite the availability of a large number of interaction measures, it is not obvious to choose the most appropriate one. The proposed procedure includes four complementary interaction measures in order to answer the previous objectives for TITO processes as the turboprop engine.

#### 3.2.1 Relative Gain Array

The well-known Relative Gain Array (RGA) developed by (Bristol, 1966) gives a suggestion on how to solve the pairing problem in the case of a decentralized controller structure. By denoting ⊗ the element-wise multiplication, the matrix RGA is given by (3). The element $RGA_{ij}$ can be seen as the quotient between the gain in the loop between input $j$ and output $i$ when all other loops are open, and the gain in the same loop when all other loops are closed. The input/output pairings corresponding to elements close to $1$ should be selected.

$$RGA = G_0 \otimes (G_0^{-1})^T \quad (3)$$

A negative element indicates that a diagonal controller with the considered loop configuration cannot guarantee the closed-loop stability.

This index provides a very simple way of choosing a loop configuration. Due to some limitations of the RGA, another measure is used to corroborate the choice of the loop configuration.

### 3.2.2 Column Diagonal Dominance

The column diagonal dominance (DD) is defined as the ratio between the gain of the diagonal element and the sum of the gain of the off-diagonal elements (4) (Maciejowski, 1989). Important $DD_i$ over 1 will indicate weak interactions. The advantage of this index is that the DD of the process is preserved when considering a decentralized controller.

$$DD_i(G(z)) = \frac{|G_{ii}(z)|}{\sum_{j\neq i}|G_{ji}(z)|} \quad (4)$$

### 3.2.3 Performance Relative Gain Array

When RGA and DD have highlighted that a decentralized control can be used with a specific control configuration, the Performance Relative Gain Array (PRGA) (5) (Hovd and Skogestad, 1992) indicates the achievable performance with a decentralized control. In the frequency region where the control is effective, the true sensitivity matrix $S$ can be defined with the decentralized sensitivity matrix $S^*$ and the PRGA (7). The following equations resume the PRGA theory:

$$PRGA\ (z) = G^*(z)G^{-1}(z) \quad (5)$$

$$S(z) = (I + G(z)K(z))^{-1}, S^*(s) = (I + G^*(s)K(s))^{-1} \quad (6)$$

$$S^*(z) \approx 0 \Rightarrow S\ (z) \approx S^*(z) PRGA\ (z) \quad (7)$$

### 3.2.4 Index $\Sigma_2$

In the case where the previous indexes have shown that a decentralized strategy was not appropriate, it is possible to use a decoupling network. The choice of its structure can be determined using the index $\Sigma_2$ (Birk and Medvedev, 2003) (8) with the $H_2$-norm computed in (9):

$$[\Sigma_2]_{ij} = \frac{\|G_{ij}\|_2}{\sum_{k,l}\|G_{kl}\|_2} \quad (8)$$

$$\|G_{ij}\|_2 = \sqrt{L_i(C) P_j L_i^T(C)} \quad (9)$$

where $L_i(C)$ is the $i^{th}$ row of the output matrix $C$ and $P_j$ the controllability gramian of the SISO subsystem. The $H_2$-norm can be interpreted as the transmitted energy between the past inputs and the future outputs. Hence, the matrix $\Sigma_2$ is suitable for quantifying the importance of the input-output channels. Indeed, each element describes the impact of the corresponding input signal on the specific output signal. The aim is to find the simplest control structure that gives a sum as close to *1* as possible.

### 3.2.5 Procedure

The proposed procedure is described in Fig. 2 for TITO processes. For a non TITO process, RGA can be replaced by the Decomposed Relative Interaction Analysis (DRIA) (He, 2004), which is more adapted to the interactions between the different loops. The Niederlinsky Index (NI) (Niederlinski, 1971) can also be used to eliminate some configurations.

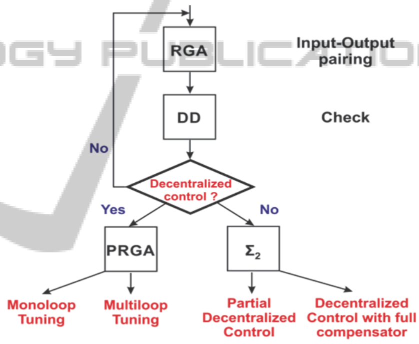


Figure 2: Procedure of interaction analysis.

## 3.3 Interaction Analysis of the Turboprop Engine

The proposed procedure is applied to the turboprop engine (after scaling it's inputs and outputs).

The RGA is first computed on each operating point. The elements corresponding to the diagonal configuration are contained between *0.9* and *1.1* and the off-diagonal elements between *-0.1* and *0.1*. The diagonal configuration is thus selected and interactions seem weak at steady-state.

In order to evaluate more precisely interactions in the turboprop engine, the inverse of the column DD of identified models is plotted in Fig. 3. The study of the column DD allows to notice that interactions are important from *WF* to *XNP* on the whole frequency domain. Interactions from $\beta$ to *SHP* are neglectable at low frequencies (which mislead the RGA) and become important around the desired bandwidth and in high frequencies.

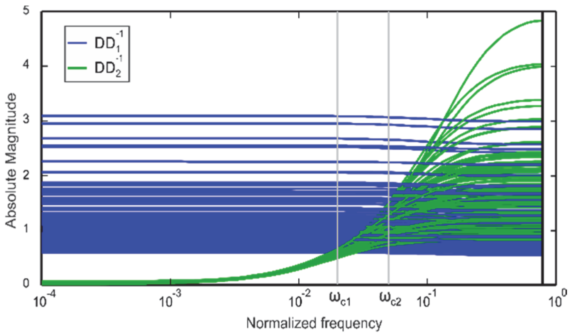

Figure 3: Column DD of the identified models.

A decentralized control is thus not viable. The $\Sigma_2$ index is calculated to determine the structure of the desired compensator. The mean of the $\Sigma_2$ matrices is presented in (10). It indicates that each transfer represents the same energy, and cannot be neglected. A full compensator is thus required.

$$\Sigma_2 = \begin{bmatrix} 22.8 & 24.8 \\ 24.6 & 27.8 \end{bmatrix} \tag{10}$$



## 4 DECOUPLING METHODS

To extend the use of decentralized controllers, decoupling techniques are used. The basic idea behind the control design based on decoupling is to find a compensator $D$ in order to obtain a *near* diagonal process $G_d$ Fig. 4. The compensator can be static (ie. constant matrix) or dynamic, ie. transfer matrix. The advantage of the static approach is that the compensator is easier to be computed and to be implemented, whereas the dynamic approach allows to lead to a better decoupling accuracy in a wider range of frequencies.

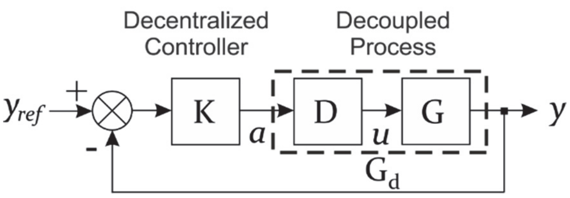

Figure 4: Decentralized controller with compensator.

### 4.1 Proposed Procedure

The choice of a decoupling method is a relatively complex task. The proposed procedure includes three methods that can lead to good results in practice.

#### 4.1.1 Static Optimization

A possible solution is to compute the optimal static compensator. In order to minimize the couplings, the column DD can be maximized. The chosen cost-function is chosen as a trade-off between the mean $DD_i^{-1}$ and the worst $DD_i^{-1}$, with the new index $\rho_i$ (11). $W$ is a frequency dependent weighting function that allows to emphasis the frequency band of interest around the desired bandwidth $w_d$ (12).

$$\rho_i = \max_k (DD_i^{-1}(G(e^{j\omega_k T_e}))) + \frac{\sum_k W(\omega_k) DD_i^{-1}(G(e^{j\omega_k T_e}))}{\sum_k W(\omega_k)} \tag{11}$$

$$W(j\omega_k) = 10 \frac{\ln\left(\left|\frac{\omega_k+\omega_d}{\omega_k-\omega_d}\right|\right)}{\max\left(\ln\left(\left|\frac{\omega_k+\omega_d}{\omega_k-\omega_d}\right|\right)\right)} \tag{12}$$

Let $L_i(G)$ be the $i^{th}$ row of $G$ and $C_j(D)$ the $j^{th}$ column of $D$. The elements of $G_d$ are given as follows:

$$G_{d_{ij}}(z) = L_i(G(z))C_j(D) \tag{13}$$

The index $DD_i$ of $G_d$ depends only on the process and the $i^{th}$ column of the compensator:

$$DD_i(G_d(z)) = \frac{|L_i(G(z))C_i(D)|}{\sum_{j\neq i}|L_j(G(z))C_i(D)|} \tag{14}$$

It is thus possible to maximise each index $\rho_i$ independently.

#### 4.1.2 Dynamic Optimization

In order to increase the degrees of freedom number of the compensator, a dynamic compensator can be computed using an extension of the previous method. Instead of a constant value, a polynomial in $z$ can be considered for each element of $D$. It is then necessary to add a common pole in order to obtain a realizable compensator.

#### 4.1.3 Inverse-based Decoupling

The easiest-to-use dynamic decoupling method is inspired by the inverse-based control approach (Gagnon et al., 1998). Three solutions are based on this concept: the ideal decoupling, the simplified decoupling and the inverted decoupling. The inverted decoupling seems to be the best solution since it regroups the advantages of the two first approaches. The principle of the inverted decoupling (Fig. 5.) is to compute the decoupler $D$ in order to ensure perfect decoupling and to keep the diagonal elements of the original process (15).

$$D = G^{-1}G^{*} \tag{15}$$

$$\begin{bmatrix} u_1 \\ u_2 \end{bmatrix} = \begin{bmatrix} G_{11} & G_{12} \\ G_{21} & G_{22} \end{bmatrix}^{-1} \begin{bmatrix} G_{11} & 0 \\ 0 & G_{22} \end{bmatrix} \begin{bmatrix} a_1 \\ a_2 \end{bmatrix} \tag{16}$$

$$\begin{bmatrix} u_1 \\ u_2 \end{bmatrix} = \begin{bmatrix} a_1 - \frac{G_{12}}{G_{11}} u_2 \\ a_2 - \frac{G_{21}}{G_{22}} u_1 \end{bmatrix} \quad (17)$$

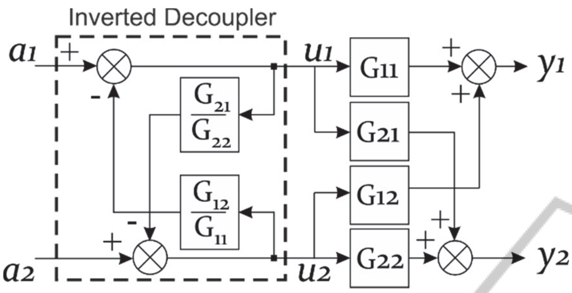


Figure 5: Scheme of the inverted decoupler.

The realizability requirement for the inverted decoupler is that all of its elements must be proper, causal and stable. In case of realizability problems, existent solutions allow to add extra dynamics or additional time delays.

### 4.1.4 Decoupling Procedure

The first step of the procedure (Fig. 6) is to compute the inverted decoupler in order to evaluate the complexity of a compensator that achieves perfect decoupling. The optimization of a static compensator and then a dynamic optimization are then applied. The order of the compensator can be increased until it reaches the complexity of the inverted decoupler. Finally, the inverted decoupler is chosen if the previous compensators do not lead to acceptable decoupling.

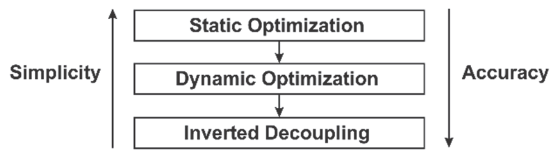


Figure 6: Procedure of decoupling.

For larger systems than TITO, the pseudo-diagonalization and the dynamic pseudo-diagonalization (Ford and Daly, 1979) can replace the optimization methods due to computation time constrains. Moreover, the inverted decoupling is not feasible for non-TITO processes, thus the simplified decoupling can be an interesting alternative.

## 4.2 Decoupling of the Turboprop Engine

Let us consider the simple form of the process given by (2), where each of the two elements of the inverted decoupler are composed of one zero and one pole (18). The requirements for the realizability of the inverted decoupler are respected. The following constraint is considered: the dynamic compensator computed by optimization shall not exceed a full first order matrix transfer.

An average model is considered in this part. The DD of this model is represented in Fig. 7. A static compensator is first researched under the form (19). Indeed, it can be noticed that multiplying one column of $D$ by a scalar does not affect the column DD nor the index $\rho_i$. It is thus possible to reduce the number of optimization parameters without limiting the degrees of freedom of the compensator. A simulated annealing optimization leads to the results presented in Table 2 and Fig. 7. Couplings being too important, a first order compensator (20) is computed. Interactions have been highly reduced, but they still remain important. The inverted decoupler is thus chosen.

$$\frac{G_{12}}{G_{11}} = \frac{K_{12}(z - z_{12})}{K_{11}(z - z_{11})} \qquad \frac{G_{21}}{G_{22}} = \frac{K_{21}(z - z_{21})}{K_{22}(z - z_{22})} \quad (18)$$

$$D = \begin{bmatrix} 1 & \beta \\ \alpha & 1 \end{bmatrix} \quad (19)$$

$$D(z) = \begin{bmatrix} 1 + \alpha_1 z & \beta_2 + \beta_3 z \\ \alpha_2 + \alpha_3 z & 1 + \beta_1 z \end{bmatrix} \quad (20)$$

Table 2: Decoupling results.

| Compensator | $\rho_1$ | $\rho_2$ |
|---|---|---|
| Normalized Process $G_n$ | 1.4 | 1.4 |
| Static optimization | 0.02 | 0.45 |
| Dynamic optimization | 0.007 | 0.21 |

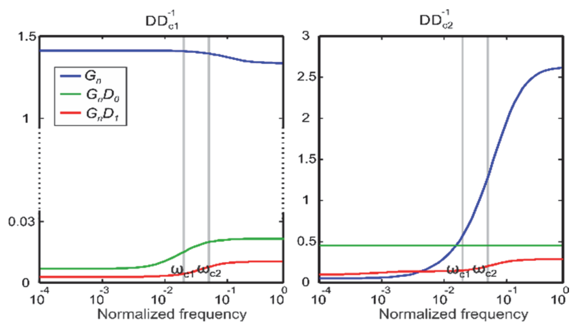


Figure 7: $DD^{-1}$ of the process and decoupled processes.

# 5 DECENTRALIZED CONTROL

Considering the dynamics of the system, PI controllers can be used. As previously mentioned, the loops are perfectly decoupled. A mono-loop design method can thus be used. The IMC-PID (Internal Model Controller) (Rivera et al., 1986) method has been chosen since it provides a suitable framework for satisfying the desired objectives. The Bode diagrams of each open-loop system (for the different operating points) are presented in Fig. 8 and compared to the desired open-loops. It can be seen that the PI tuning allows having a behavior close to the technical specifications.

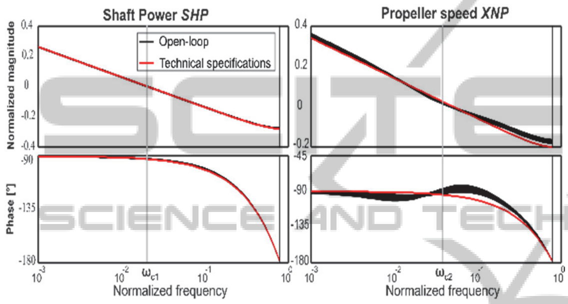


Figure 8: Bode diagrams of the open-loop system.

# 6 ROBUSTNESS ANALYSIS

Generally, when talking about industrial processes, a model never perfectly represents the real plant to be controlled. Consequently, it is necessary to deal with associated model uncertainties. These correspond, either to uncertainties in the physical parameters of the plant or to neglected dynamics. In this context, the issue is to validate a control law by analysing its stability robustness and performance properties. The structured singular value approach has been selected because it provides a general framework to robustness analysis problem (Ferreres, 1999).

## 6.1 Uncertain Turboprop Engine under an LFT Form

The main issue is to transform the closed-loop subject to model uncertainties into the standard interconnection structure. Uncertainties can be considered on each of the eight parameters of the identified model (under state-space representation). In order to have meaningful uncertainties, it has been chosen to define them as percentage of their possible range on the set of identified models (21), (22).

$$A_{ij} = A_{ij0} + x\,\% \times (A_{ij\sup} - A_{ij\inf})\delta_{A_{ij}} \quad (21)$$

$$B_{ij} = B_{ij0} + x\,\% \times (B_{ij\sup} - B_{ij\inf})\delta_{B_{ij}} \quad (22)$$

Moreover, some dynamics could have been neglected during the modelling or the identification steps. Neglected dynamics are thus introduced at the plant inputs: first order filters (with bandwidth five times greater than the desired bandwidths) are considered for each loop. The turboprop engine under LFT (Linear Fractional Transformation) form is represented in Fig. 9.

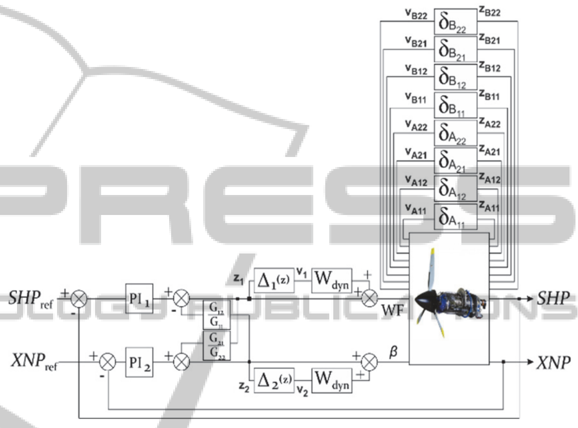


Figure 9: Turboprop engine under LFT form.

## 6.2 Results

Uncertainties of 25% of the parameters' ranges are considered to evaluate the robustness of the stability. The maximum of the upper bounds of the singular values (noted VSSM) are represented in the Fig. 10. Each value is represented depending on the Mach number, the altitude and the engine speed of turboprop engine. Except three points that present maximum singular values over 1.5, control laws can tolerate an uncertainty average of 25%.

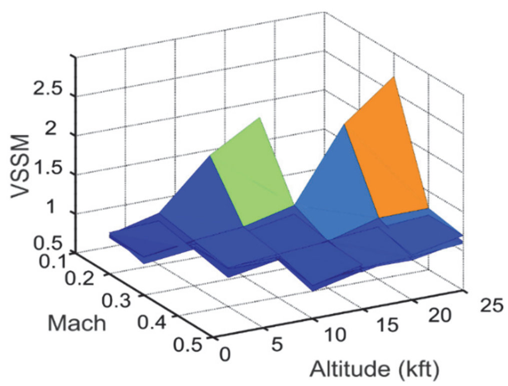


Figure 10: Upper bounds of the singular values (stability).

In order to test the performances robustness, an additional (fictitious) performance block is added to the model perturbation. This last includes two dynamics and allows ensuring modulus margins of 0.4. Uncertainties of 10% of the ranges of the parameters are considered. The maximum of the upper bounds of the singular values are represented in the Fig. 11. Except the same three points of the previous case, the control laws maintain their performances in terms of set-point tracking and margin stability with an uncertainty average of 10%.

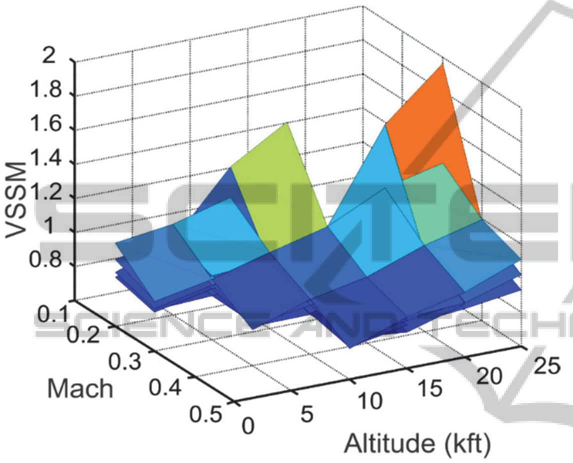


Figure 11: Upper bounds of the singular values (set-point tracking and modulus margin).

The control laws for the three operating points previously mentioned have been re-designed, with poorer nominal performances but better robust performances. The mu-analysis have demonstrate that the control laws were robust to 10% uncertainties. Even if these results are satisfactory, the control laws designed in one operating point are not able to ensure the desired performances on the whole flight envelope, hence the need of an interpolation strategy.

## 6.3 Interpolation

In order to guarantee the desired performances over the whole flight envelope, control laws need to be interpolated. Each parameter of the control laws is interpolated individually by a gain scheduling technique. Moreover an incremental algorithm (also called velocity algorithm) is used to ensure bumpless parameter changes. The algorithm first computes the change rate of the control signal which is then fed to an integrator (Åström and Hägglund, 1995). Finally, Fig. 12 presents the control laws in their final configuration.

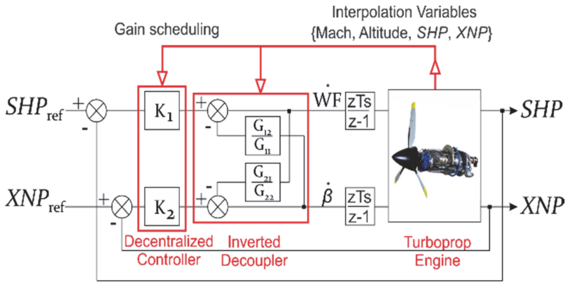


Figure 12: Control laws implemented with an incremental algorithm.

# 7 SIMULATION RESULTS

Control laws, associated to the PI controllers and the inverted decoupler, have been finally implemented on the non linear model of the turboprop engine. The validation scenario includes successive reference steps, perturbations and noise. Simulation results are plotted in Fig. 13 and in Fig. 14. The time responses are in agreement with the specified bandwidths (considering the limitations on commands and their derivatives). Moreover, overshoots are not important and there are no steady-state errors. Some peaks are noticed on the propeller speed when there are important steps on the shaft power, but they are quickly corrected. Technical specifications are thus respected, condition needed in order to validate the control laws.

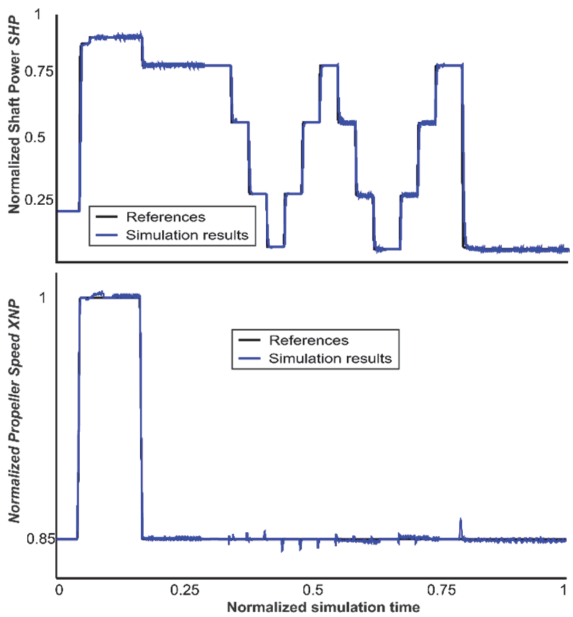


Figure 13: Simulation results.

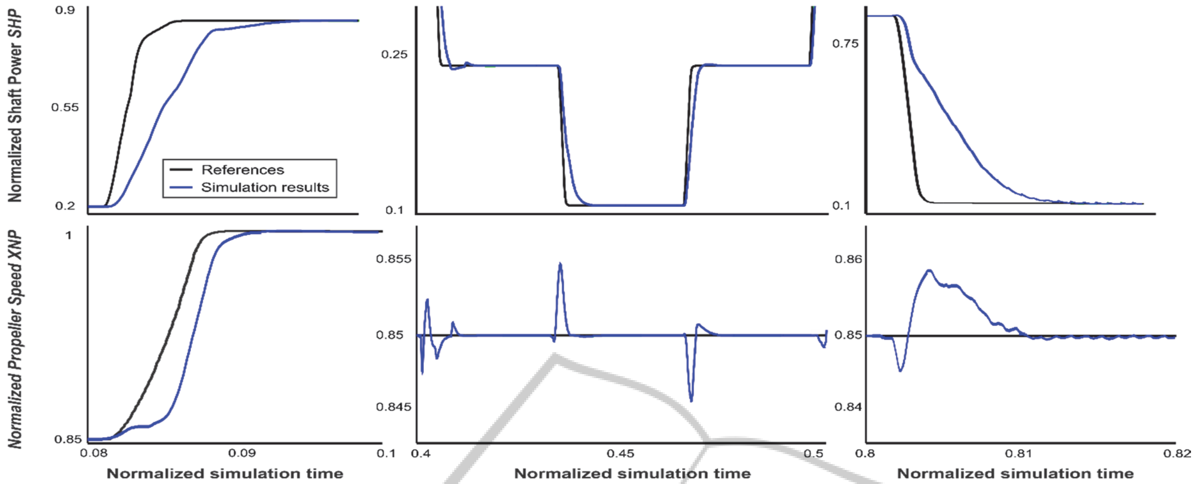


Figure 14: Simulation results (zoom on some transient states).

## 8 CONCLUSIONS

This paper proposes a straightforward and systematic way of designing a decentralized control. The first step consists in analyzing the interactions of the process. The proposed procedure leads the choice of an input-output pairing and a control strategy. Given the high couplings of the turboprop engine, an inverted decoupler has been used to reduce the interactions. PI controllers have then been tuned using an IMC-PID method.

Control laws have been interpolated using a gain scheduling method in order to ensure the desired performances on the flight envelope. Robustness analysis and simulation results finally illustrate the *good* performances of the control laws.

Future works will focus on the adaptation of the proposed methodology in order to take into account the uncertainties during the interaction analysis and the decoupling steps.

## REFERENCES

Âström, K.J., Hägglund, T., 1995. *PID Controllers: Theory, Design, and Tuning, 2nd edition*. ISA.

Birk W., Medvedev. A., 2003. "A note on gramian-based interaction measures". Proc. European Control Conference, Cambridge, UK.

Bristol, E., 1966. "On a new measure of interactions for multivariable process. Automatic Control". IEEE Transactions on, Vol 11(1) pp 133-134.

Ferreres, G., 1999. *A practical approach to robustness analysis with aeronautical applications*. Kluwer Academic Publishers.

Ford M.P., Daly K.C., 1979. "Dominance improvement by pseudodecoupling". Proceedings of the Institution of Electrical Engineers. Vol 126(12) pp 1316-1320.

Gagnon, E., Pomerleau, A., Desbiens, A., 1998. "Simplified, ideal or inverted decoupling?". ISA Trans. Vol 37, pp. 265-276.

Garrido, J., Vasquez, F., Morilla F., 2011. "Generalized Inverted Decoupling for TITO processes". IFAC, Milano, Italy.

He M.J., C. W., 2004. "New Criterion for Control-Loop Configuration of Multivariable Processes". Control, Automation, Robotics and Vision Conference, Vol 2, pp 913-918.

High, G.T., Prevallet, L.C., Free, J.W., 1991. "Apparatus for decoupling a torque loop from a speed loop in a power management system for turboprop engines". US 5274558 A.

Hovd M., Skogestad. S., 1992. "Simple frequency-dependent tools for control system analysis, structure selection and design". Automatica, Vol 28(5) pp 989-996.

Le Brun, C., Godoy, E., Beauvois D., Liacu, B., Noguera, R., 2014. "Control Laws Design of a Turboprop Engine". Applied Mechanics and Materials Vol 704 pp 362-367.

Maciejowski J.M., 1989. *Multivariable Feedback Design*. Addison Wiley.

Niederlinski, A., 1971. "A heuristic approach to the design of linear multivariable interacting control systems". Automatica, Vol 7 pp 691-701.

Rivera, D.E., Morari, M., Skogestad, S., 1986. *Internal model control. 4. PID controller design*. Ind. Eng. Chem. Process Des. Dev., 25, pp 252.

Snecma, 2012. *Training Manual Turboprop - General Familiarization*.

Soares, C., 2008. *Gas Turbines: a Handbook of Air, Land and Sea Application*. Butterworth-Heinemann.